

Argon isotopic composition of Archaean atmosphere probes early Earth geodynamics

Magali Pujol¹, Bernard Marty¹, Ray Burgess², Grenville Turner² and Pascal
Philippot³

¹ CRPG-CNRS, Université de Lorraine, 15 rue Notre Dame des Pauvres, 54501 Vandoeuvre-
lès-Nancy Cedex, France

² School of Earth, Atmospheric and Environmental Sciences, University of Manchester,
Oxford Road, Manchester, M13 9PL, United Kingdom.

³ Institut de Physique du Globe de Paris, Sorbonne-Paris Cité, Université Paris Diderot,
CNRS, 1 rue Jussieu 75238 Paris Cedex 5, France.

(Corresponding Author: bmarty@crpg.cnrs-nancy.fr)

Understanding the growth rate of the continental crust through time is a fundamental issue in Earth sciences¹⁻⁸. The isotopic signatures of noble gases in the silicate Earth (mantle, crust) and in the atmosphere permit exceptional insight into the evolution through time of these reservoirs⁹. However, no data for such compositions exists for the distant past, and temporal exchange rates between the Earth's interior and its surface are severely under-constrained due to a lack of samples preserving the original signature of the atmosphere at the time of their formation. Here, we report the analysis of argon in 3.5 Ga-old hydrothermal quartz. Noble gases are hosted in primary fluid inclusions containing a mixture of Archaean freshwater and hydrothermal fluid. Our component analysis shows the occurrence of Archaean atmospheric argon having a lower $^{40}\text{Ar}/^{36}\text{Ar}$ (143 ± 24 , 3.5 Ga ago) than the present-day value (where ^{40}Ar has been produced by the radioactive decay of ^{40}K which has a half-life of 1.25 Ga, and ^{36}Ar is primordial in origin). This ratio is consistent with an early development of the felsic crust, which might have played an important role in climate variability during the first half of the Earth's history.

The continents formed by extraction of incompatible elements from the mantle such as those producing radiogenic heat (U, Th, ^{40}K). The extracted elements have been stored at the Earth's surface since the crust is buoyant, that is, less dense than the underlying mantle. Consequently, the development of the continents impacted the composition of the mantle and also shaped the thermal regime of the silicate Earth. Yet no consensus exists on the mode of formation and on the growth rate of the crust. Geological units formed during the first Ga are scarce, and geochemical methods available to model crustal evolution such as Sm-Nd of shales⁷, U-Pb and Hf isotopes of zircons^{1,8} may have difficulties in distinguishing between reworking of already existing crust and creation of juvenile crust (although a combination of isotope tracers seems to provide better constraints¹).

The terrestrial atmosphere has evolved due to volatile exchange between the mantle and the surface of our planet. The inert gases in the atmosphere have accumulated for eons and have kept an integrated memory of the degassing of the mantle and the crust. Argon isotopes are potentially useful tracers of these exchanges⁹: ³⁶Ar is primordial, and has been thoroughly degassed from the mantle early in Earth history, whereas ⁴⁰Ar, in negligible amount at the time of terrestrial accretion, has been produced by the decay of ⁴⁰K. Presently ⁴⁰Ar is the most abundant argon isotope in the atmosphere (the atmospheric ⁴⁰Ar/³⁶Ar = 298.6¹⁰), a robust indication of terrestrial degassing through time. The atmosphere contains 1.65 x 10¹⁸ moles of ⁴⁰Ar¹¹, which corresponds to about half of the total ⁴⁰Ar produced in the solid Earth (4.0 x 10¹⁸ mol ⁴⁰Ar for a silicate Earth K content of 280 ppm¹²). The mantle has been evolving through convection and partial melting, during which argon was degassed from mantle-derived magmas into the hydrosphere and atmosphere, while potassium was concentrated into magmas due to its incompatible nature, and in-part stored in the continental crust. As soon as the continental crust was formed, even partially, produced radiogenic ⁴⁰Ar was less easily degassed into the atmosphere. Consequently, the atmospheric ⁴⁰Ar/³⁶Ar ratio has the potential to trace not only mantle activity but also the growth of the continental crust¹³, and to constrain the numerous models of mantle-atmosphere evolution that have been proposed¹⁴⁻¹⁷. Unfortunately, the record of ancient atmospheric argon isotope ratios in sedimentary rocks is severely compromised by subsequent *in situ* ⁴⁰Ar production as well as by interaction with crustal fluids containing ⁴⁰Ar from fluid-rock interaction. Only two attempts to measure ancient atmosphere in a single sedimentary rock appear to have been unaffected by the presence of excess ⁴⁰Ar. Cadogan¹⁸ and Rice et al.¹⁹ proposed that the ⁴⁰Ar/³⁶Ar ratio of the atmosphere in the 395 Ma Rhynie chert, NE Scotland, was 294.1 ± 1.5 (re-normalized to a present day value of 298.56±0.31¹⁰). This temporal change requires a ⁴⁰Ar flux of 6.2±2.1 x 10⁷ mol/yr from the solid Earth (crust+mantle) to the atmosphere averaged

over the last 400 Ma, which is consistent with a contemporaneous ^{40}Ar flux of $11 \pm 1 \times 10^7$ mol/yr estimated from measurements of atmospheric argon trapped in Antarctic ice over a time period of 780 Ka²⁰.

Our sample comes from the 3.5 Ga-old Dresser Formation (Warrawoona Group, Pilbara Craton) at North Pole, Western Australia. This formation comprises metabasalts and metakomatiites interleaved with three beds of cherty metasediments that have experienced low-grade metamorphism²¹. The lowermost unit is intercalated with several barite beds and is overlain by silicified carbonate. Undeformed pillow basalts are found above the contact with the chert-barite horizon. Some of the pillow basalts host isolated quartz-carbonate aggregates forming pods. The studied sample is from one of these pods which resemble typical mineralisation associated with passive hydrothermal circulation of water through shallow crust. Intrapillow quartz crystals contain abundant, 1-25 μm , two phase (liquid and <5% vapor) aqueous inclusions, [that have been extensively studied for their chemistry](#)²². Fluid inclusions are randomly distributed throughout the host quartz, which argues for a primary origin. The absence of crosscutting veins, metamorphic overprint, and deformation features affecting basalt pillows and associated pods indicates negligible fluid remobilization and circulation after deposition and crystallization.

The argon and xenon abundances and isotopic compositions, together with K and Cl contents, were measured by vacuum stepwise crushing, followed by stepwise heating [of the powder remaining after crushing](#), using the extended Ar-Ar method²³ ([Tables A1 & A2](#), Supplementary Information). With this method, samples were irradiated [before analysis](#) with neutrons to transform ^{35}Cl , ^{37}Cl and ^{39}K to ^{36}Ar , ^{38}Ar and ^{39}Ar , respectively, in order to determine the Cl and K contents on the same extraction steps as ^{36}Ar and ^{40}Ar . Our crushing step data (Table A1) confirm the presence of hydrothermal fluids that were previously identified by X-ray microfluorescence²²: the Cl/K ratios from crushing experiments vary

between 3.6 and 9.4 (Figure A1, Supplementary Information), within the range of 2-48 previously observed²².

The $^{40}\text{Ar}/^{36}\text{Ar}$ and $\text{Cl}/^{36}\text{Ar}$ ratios clearly correlate (Fig. 1) between a component rich in radiogenic ^{40}Ar and chlorine and having a near-constant $\text{Cl}/^{40}\text{Ar}$ ratio of 3245 ± 330 (Supplementary Information), and a second component with low $^{40}\text{Ar}/^{36}\text{Ar}$ and low $\text{Cl}/^{36}\text{Ar}$ values. Because potassium was also measured in these extractions, we compute how much ^{40}Ar could have been produced in-situ ($^{40}\text{Ar}_{\text{IS}}$) by ^{40}K decay during 3.5 Ga (Table A1). This accumulation can account for only 5% at best of total ^{40}Ar for the crushing steps, and 25-34% for the heating steps. Thus the correlation of Fig. 1 indicates mixing between a low $^{40}\text{Ar}/^{36}\text{Ar}$, low salinity component that we regard as water containing dissolved atmospheric gases, and an hydrothermal fluid end-member containing excess ^{40}Ar ($^{40}\text{Ar}_{\text{HY}}$), in constant proportion with respect to Cl. The component displaying low Cl contents and low $^{40}\text{Ar}/^{36}\text{Ar}$ ratios also has low Cl/K ratios (<2 ; Fig. A1, Supplementary Information), and is most apparent in the stepwise heating release of gases from the crushed samples, possibly preserved in micrometric fluid inclusions (Fig. 1). The low Cl/K ratio cannot be explained by a simple dilution of the hydrothermal fluids released during sample crushing, nor by the occurrence of a seawater component ($\text{Cl}/\text{K} = 57$ for modern seawater). It is instead consistent with the occurrence of a paleo-atmospheric end-member dissolved in freshwater.

An estimate of the atmospheric $^{40}\text{Ar}/^{36}\text{Ar}$ ratio can be derived from the intercept of the correlation shown in Fig. 1. However, the data must also be corrected for $^{40}\text{Ar}_{\text{IS}}$. Since K is measured for all crushing and heating steps, the correction only requires knowledge of the time of argon trapping in the sample. The Dresser formation is well dated at 3.52 Ga by the U-Pb method²⁴, at 3.5 Ga by the Sm-Nd method²⁵, and at 3.49 Ga by the Pb-Pb method²⁶. Massive barite from the Dresser formation has a U-Xe_f (Xe_f represent xenon isotopes produced by the natural fission of ^{238}U) age of 3.7 ± 0.5 Ga²⁷ and contains excesses of ^{130}Xe

($^{130}\text{Xe}^*$) from the double electron capture decay of ^{130}Ba ($T_{1/2} = 6 \times 10^{20}$ a) in both fluid inclusions and in the matrix, that demonstrate the antiquity of trapped noble gases²⁷. Ar-Ar dating of trapped fluids could not be directly determined for the present sample due to the large contribution of inherited Ar, but we present in the Methods section an Ar isotope data analysis that suggests strongly that fluids trapped in the samples are ≥ 2.7 Ga, probably as old as the Dresser unit. Further evidence that hydrothermal quartz can store noble gases over Ga timescales arises from the study of another hydrothermal quartz sample filling vacuoles in the komatiitic basaltic unit in the Dresser formation. In that sample, in-situ radiogenic Ar dominates over the hydrothermal and atmospheric components²⁸, and yields a Ar-Ar plateau age of 3.0 ± 0.2 Ga²⁸. Both that sample²⁸ and the one studied here (Supplementary Information) have radiogenic $^{130}\text{Xe}^*$ from the decay of very long-lived ^{130}Xe , and the stable isotope composition of trapped xenon appears fractionated (that is, enriched in the light isotopes compared to the modern atmospheric Xe, Table A2 and Fig. A3, Supplementary Information), a signature of paleo-atmospheric xenon from the Archean eon²⁸. The last regional metamorphic event took place 2.7 Ga ago, after which the terranes have been thermally and tectonically stable up to the present²¹. These different lines of evidence, including the textural ones presented above for a primary origin of fluid inclusions, indicate an Archean age for fluids trapped in this sample, consistent with the formation age of 3.5 Ga, with a possible lower limit of 2.7 Ga.

After correction for radiogenic ^{40}Ar , the intercept of the mixing correlation yields an Archean atmospheric $^{40}\text{Ar}/^{36}\text{Ar}$ ratio of 143 ± 24 (95 % conf. int., MSWD = 1.5) for $t = 3.5$ Ga, obtained using an error-weighted York's regression²⁹. Assuming younger fluid ages of 3.0 Ga and 2.7 Ga, the initial $^{40}\text{Ar}/^{36}\text{Ar}$ ratios are 189 ± 21 and 211 ± 21 , respectively. The first heating step at 400°C released argon with $^{40}\text{Ar}/^{36}\text{Ar} = 305 \pm 13$, which is consistent with the modern atmospheric $^{40}\text{Ar}/^{36}\text{Ar}$ ratio (298.6 ± 0.3^{10}), and could indicate modern atmospheric

contamination. Although during this step ^{39}Ar from neutron irradiation of ^{39}K was also released, suggesting that trapped argon was released at this temperature, we attempted regressions without the 400°C data, which yielded Archean atmospheric $^{40}\text{Ar}/^{36}\text{Ar}$ ratios of 143 ± 29 (3.5 Ga), 190 ± 28 (3.0 Ga) and 212 ± 27 (2.7 Ga). These values are undistinguishable from those obtained by including the 400°C step, demonstrating that the results do not depend the low temperature step data.

We have developed a first order rate box model following Hamano & Ozima⁹, in which the mantle degasses Ar isotopes into the atmosphere through geological time. Potassium is extracted from the mantle during partial melting and is retained in majority in the developing continental crust. The boxes are the mantle, the crust which accumulates K and the atmosphere. The variables are the mantle extraction rate, the crustal degassing rate for ^{40}Ar (characterized by a β parameter⁹ varying between 0.05, representing almost no crustal degassing, and 0.37, corresponding to 50% crustal degassing, ref. 9 for justification) and the fraction of early degassed ^{36}Ar . The constraints of the model applied to validate the possible solutions are the present-day mantle $^{40}\text{Ar}/^{36}\text{Ar}$ ratios (5,000 and 40,000 for mantle plume and mid-ocean ridge basalt sources, respectively), the $^{40}\text{Ar}/^{36}\text{Ar}$ ratio of the modern atmosphere of 298.6^{10} , the paleoatmospheric $^{40}\text{Ar}/^{36}\text{Ar}$ values determined above, the fraction of bulk silicate Earth K present in the present-day continental crust (between 20% and 50%¹²), and the mean ^{40}Ar flux to the atmosphere in the last 400 Ma¹⁸, representing modern conditions. Hundreds of tests run with this model gave all possible solutions matching modern conditions and the range of Archean atmosphere $^{40}\text{Ar}/^{36}\text{Ar}$ ratios (Supplementary Information). The best solutions indicate that: (i) catastrophic mantle degassing during the first 170 Ma (impact degassing of accreting bodies cannot be differentiated here); (ii) between 170 Ma and 3.8 Ga, less than 10 % stable felsic crust; (iii) between 3.8 Ga and 2.5 Ga, formation of a crustal volume equivalent to 80 ± 10 % of the present-day one; (iv) between 2.5 Ga and present-day,

less than 30 % crustal generation, consistent with possible reworking of previously emplaced felsic crust¹.

The extraction of a large reservoir of felsic crust during the Archaean eon modified profoundly the thermal regime of the Earth by storing heat-producing radio-elements at the surface. It might have been instrumental to decrease the partial pressure of atmospheric CO₂, via alteration of this juvenile crust, from high contents of several percents necessary to prevent Earth's surface from total freezing when the Sun was ~25 % less energetic (eg., ³⁰), to a few hundreds of ppm that allowed snowball Earth episodes in the late Archaean.

Methods Summary

We selected quartz because of its generally low content of noble gas-producing elements (e.g., K and U). The sample was first neutron-irradiated (to obtain, in addition to natural Ar isotopes, the Cl and K contents), then progressively crushed, and the resulting powder was heated in several temperature steps. ³⁶Ar is predominantly from the atmosphere, but ⁴⁰Ar can be contributed by three sources, the atmosphere, "excess" ⁴⁰Ar from the hydrothermal component (⁴⁰Ar_{HY}) and ⁴⁰Ar produced in-situ (⁴⁰Ar_{IS}) from the in-situ decay of ⁴⁰K. To determine the atmospheric ⁴⁰Ar/³⁶Ar ratio, the measured ⁴⁰Ar content needs to be corrected for contributions of ⁴⁰Ar_{HY} and ⁴⁰Ar_{IS}. Evaluating the latter requires only knowledge of the age since K is also measured. In addition to geological and geochemical evidences presented in the main text, we have applied a statistical approach that confirms the Archaean age of the trapped fluids. We first correct for the hydrothermal contribution. The hydrothermal Cl/⁴⁰Ar_{HY} ratio is obtained from the analysis of the crushing runs which are dominated (≥95%) by this component (Table A3). The step-heating run data are corrected for hydrothermal contribution by subtracting the step-heating Cl contents multiplied by the Cl/⁴⁰Ar_{HY} ratio obtained above. The assumption that the Cl/⁴⁰Ar_{HY} ratio of the step-heating

and crushing runs are similar is justified by the unique slope of the Fig. 1 correlation. Corrected step-heating data define several equations (one per temperature step) with two unknowns, the amount of in-situ produced ^{40}Ar which depends on fluid age, and the initial (atmospheric) $^{40}\text{Ar}/^{36}\text{Ar}$ ratio. We explored the sets of ages and initial $^{40}\text{Ar}/^{36}\text{Ar}$ values that fit best the equations and found that they correspond to ages around 3.5 Ga (Methods, Table A3 and Fig. A2 in Supplementary Information). These ages were then used to correct for $^{40}\text{Ar}_{\text{IS}}$ the regression shown in Fig. 1. The initial, presumably paleo-atmospheric $^{40}\text{Ar}/^{36}\text{Ar}$ ratio was computed using the error-weighted regression method of York²⁹.

200

201 **References**

- 202 1. Dhuime, B., Hawkesworth, C.J., Cawood, P.A. & Storey, C.D. A Change in the
203 geodynamics of continental growth 3 billion years ago. *Science* **335**, 1334-1336 (2012).
- 204 2. Hawkesworth, C. J. & Kemp, A. I. S. The differentiation and rates of generation of the
205 continental crust. *Chem. Geol.* **226**, 134-143 (2006).
- 206 3. Armstrong, R. L. & Harmon, R.S. Radiogenic isotopes: the case for crustal recycling on a
207 near-steady-state no-continental-growth Earth. *Phil. Trans. R. Soc. Lond. A* **301**, 443-472
208 (1981).
- 209 4. Hurley, P.M. & Rand, J.R. Pre-drift continental nuclei. *Science* **164**, 1229-1242 (1969).
- 210 5. McLennan, S.M. & Taylor, R. S. Geochemical constraints on the growth of the continental
211 crust. *J. Geol.* **90**, 347-361 (1982).
- 212 6. Reymer, A. & Schubert, G. Phanerozoic addition rates to the continental crust and crustal
213 growth. *Tectonics* **3**, 63-77 (1984).
- 214 7. Allègre, C.J. & Rousseau, D. The growth of the continent through geological time studied
215 by Nd isotope analysis of shales. *Earth Planet. Sci. Lett.* **67**, 19–34 (1984).
- 216 8. Condie, K.C., Bickford, M.E., Aster, R.C., Belousova, E. & Scholl, D.W. Episodic zircon
217 ages, Hf isotopic composition, and the preservation rate of continental crust. *Geol. Soc. Am.*
218 *Bull.* **123**, 951-957 (2011).

- 219 9. Hamano, Y. & Ozima, M. Earth-Atmosphere Model Based on Ar Isotopic Data. in:
220 Terrestrial Rare Gases, EC Alexander and M. Ozima, eds., *Adv. Earth Planet. Sci., Jpn. Sci.*
221 *Soc.* **3**, 155-171 (1978).
- 222 10. Lee, J.-Y. & al. A redetermination of the isotopic abundances of atmospheric Ar.
223 *Geochim. Cosmochim. Acta* **70**, 4507-4512 (2006).
- 224 11. Ozima, M. & Podosek, F.A. Noble Gas Geochemistry, *Cambridge Univ. Press*,
225 Cambridge, U.K. (2001).
- 226 12. Arevalo Jr. R., McDonough, W.F. & Luong, M. The K/U ratio of the silicate Earth:
227 Insights into mantle composition, structure and thermal evolution. *Earth Planet. Sci. Lett.*
228 **278**, 361-369 (2009).
- 229 13. Fanale, F.P. A case for catastrophic early degassing of the Earth. *Chem. Geol.* **8**, 79-105
230 (1971).
- 231 14. Pepin, R.O. Atmospheres on the terrestrial planets: Clues to origin and evolution. *Earth*
232 *Planet. Sci. Lett.* **252**, 1-14 (2006).
- 233 15. Tolstikhin, I.N. & Marty, B. The evolution of terrestrial volatiles: a view from helium,
234 neon, argon and nitrogen isotope modeling. *Chem. Geol.* **147**, 27-52 (1998).
- 235 16. Porcelli, D. & Wasserburg, G.J. Mass transfer of helium, neon, argon, and xenon through
236 a steady-state upper mantle. *Geochim. Cosmochim. Acta*, 59 (23), 4921-4937 (1995).
- 237 17. Allègre, C. J., Staudacher, T. & Sarda, P. Rare gas systematics: formation of the
238 atmosphere, evolution and structure of the Earth's mantle. *Earth Planet. Sci. Lett.* **81**, 127-150
239 (1987).
- 240 18. Cadogan, P. H. Paleoatmospheric argon in Rhynie chert. *Nature* **268**, 38-41 (1977).

- 241 19. Rice, C. M. et al. A Devonian auriferous hot spring system, Rhynie, Scotland. *J. Geol. Soc.*
242 *Lond.* **152**, 229-250 (1995).
- 243 20. Bender, et al.. The contemporary degassing rate of Ar-40 from the solid Earth. *Proc.. Nat.*
244 *Acad. Sci. USA* **105**, 8232-8237 (2008).
- 245 21. Buick, R. & Dunlop, J. S. R. Evaporitic sediments of early Archaean age from the
246 Warrawoona Group, North Pole, Western Australia. *Sedimentology* **37**, 247-277 (1990).
- 247 22. Foriel, J. et al. Biological control of Cl/Br and low sulfate concentration in a 3.5-Ga-old
248 seawater from North Pole, Western Australia. *Earth Planet. Sci. Lett.* **228**, 451-463 (2004).
- 249 23. Turner, G. Hydrothermal fluids and argon isotopes in quartz veins and cherts. *Geochim.*
250 *Cosmochim. Acta* **52**, 1443-1448 (1989b).
- 251 24. Van Kranendonk, M. J., Philippot, P., Lepot, K., Bodorkos, S. & Parajno, F. Geological
252 setting of Earth's oldest fossils in the ca. 3.5 Ga Dresser Formation, Pilbara Craton, Western
253 Australia. *Precamb. Res.* **167**, 93-124 (2008).
- 254 25. Tessalina, S.G., Bourdon, B., Van Kranendonk, M.V., Birck, J.L. & Philippot, P.
255 Influence of Hadean crust evident in basalts and cherts from the Pilbara Craton. *Nature*
256 *Geosci.* **3**, 214-217 (2010)
- 257 26. Thorpe, R.I., Hickman, A.H., Davis, D.W., Mortensen, J.K. & Trendall, A.F. U-Pb zircon
258 geochronology of Archaean felsic units in the Marble Bar region, Pilbara Craton, Western
259 Australia. *Precamb. Res.* **56**, 169-189 (1992).
- 260 27. Pujol, M., Marty, B., Burnard, P., & Philippot, P. Xenon in Archaean barite: Weak decay
261 of ¹³⁰Ba, mass-dependent isotopic fractionation and implication for barite formation.
262 *Geochim. Cosmochim. Acta* **73**, 6834-6846 (2009).

28. Pujol, M., Marty, B. & Burgess, R. Chondritic-like xenon trapped in Archaean rocks: a possible signature of the ancient atmosphere. *Earth Planet. Sci. Lett.* **308**, 298-306 (2011).
29. York, D. Least-squares fitting of a straight line. *Can. J. Phys.* **44**, 1079-1086 (1966).
30. Kasting, J. F. Faint young Sun redux. *Nature* **464**, 687-689 (2010).

Acknowledgements

We thank Dave Blagburn and Laurent Zimmermann for their technical support with the irradiated samples measurements, and Morvan Derrien and Benoît Faure for their help on the conception of the degassing model. This project was funded by the CNRS, the Région Lorraine, the ANR (Agence Nationale pour la Recherche) projects "e-Life" and "e-Life2" to PP and by the European Research Council under the European Community's Seventh Framework Program (FP7/2007–2013 grant agreement no. 267255 to BM. The drilling program was supported by funds from the Institut de Physique du Globe de Paris (IPGP) and the CNRS, and by the Geological Survey of Western Australia (GSWA). We thank three referees for their constructive comments. In particular, one referee helped us considerably to improve the clarity of this ms. CRPG contribution n° 2239.

Authors' contributions

MP and RB performed the experiments and analyzed the data. PP provided the sample and characterized the fluid inclusions. MP and BM did the calculations, the modeling, and wrote the paper. All of authors commented on the manuscript.

Figures

Figure 1: $^{40}\text{Ar}/^{36}\text{Ar}$ vs. $\text{Cl}/^{36}\text{Ar}$ for step-heating and step-crushing data of the irradiated sample (top : all data; bottom : enlargement on the stepwise heating data). Data define a two-component mixing trend between an hydrothermal end-member rich in chlorine and inherited $^{40}\text{Ar}_{\text{HY}}$, and a low $^{40}\text{Ar}/^{36}\text{Ar}$, $\text{Cl}/^{36}\text{Ar}$ end-member representative of low salinity water component containing dissolved atmospheric gases. The open symbols represent data from Table A1, and the red symbols represent data corrected for in-situ production of radiogenic ^{40}Ar since the time of fluid trapping (dotted line and solid line, error-weighted regressions of uncorrected, and age-corrected data, respectively). Here an age of 3.5 Ga has been taken, and the regression line²⁹ for age-corrected data yields $^{40}\text{Ar}/^{36}\text{Ar} = 143 \pm 24$ (95 % conf. int.) for the Archaean atmosphere at 3.5 Ga. Taking other possible ages of 3.0 Ga and 2.7 Ga (see text and Methods for justification) will change the $^{40}\text{Ar}/^{36}\text{Ar}$ values to 189 ± 21 and 211 ± 21 , respectively. These different possible values are also used in the atmospheric $^{40}\text{Ar}/^{36}\text{Ar}$ evolution and crustal growth model shown in Fig. 2.

Figure 2: Evolution of the atmospheric $^{40}\text{Ar}/^{36}\text{Ar}$ ratio and of the volume of continental crust relative to its present-day volume, as a function of time. A- atmospheric $^{40}\text{Ar}/^{36}\text{Ar}$ vs. time obtained with our box model described in the Supplementary Information. The shadowed areas integrate the trajectories of atmospheric $^{40}\text{Ar}/^{36}\text{Ar}$ ratio through time for the two extreme rates of crustal degassing ($\beta=0.05$ corresponds to less than 1% crust degassing rate and $\beta=0.37$ corresponds to 50% crust degassing rate⁹). Only the corresponding model runs that match our inferred $^{40}\text{Ar}/^{36}\text{Ar}$ range of values for Archaean atmospheric argon and ages (shown as vertical bars) on one hand, and the boundary conditions presented in Table A3 on another hand, are represented. B- Crust fraction vs. Time. Evolution of the volume of continental crust through time, represented as a fraction of the present-day volume. The shadowed areas integrate the model runs that fit the conditions defined above. Note that the different boundary conditions we tested (ages of 3.5 Ga, 3.0 Ga and 2.7 Ga, corresponding initial $^{40}\text{Ar}/^{36}\text{Ar}$ ratios of 143 ± 24 , 189 ± 21 , and 211 ± 21 , respectively) yield essentially the same evolution curve for crustal growth.

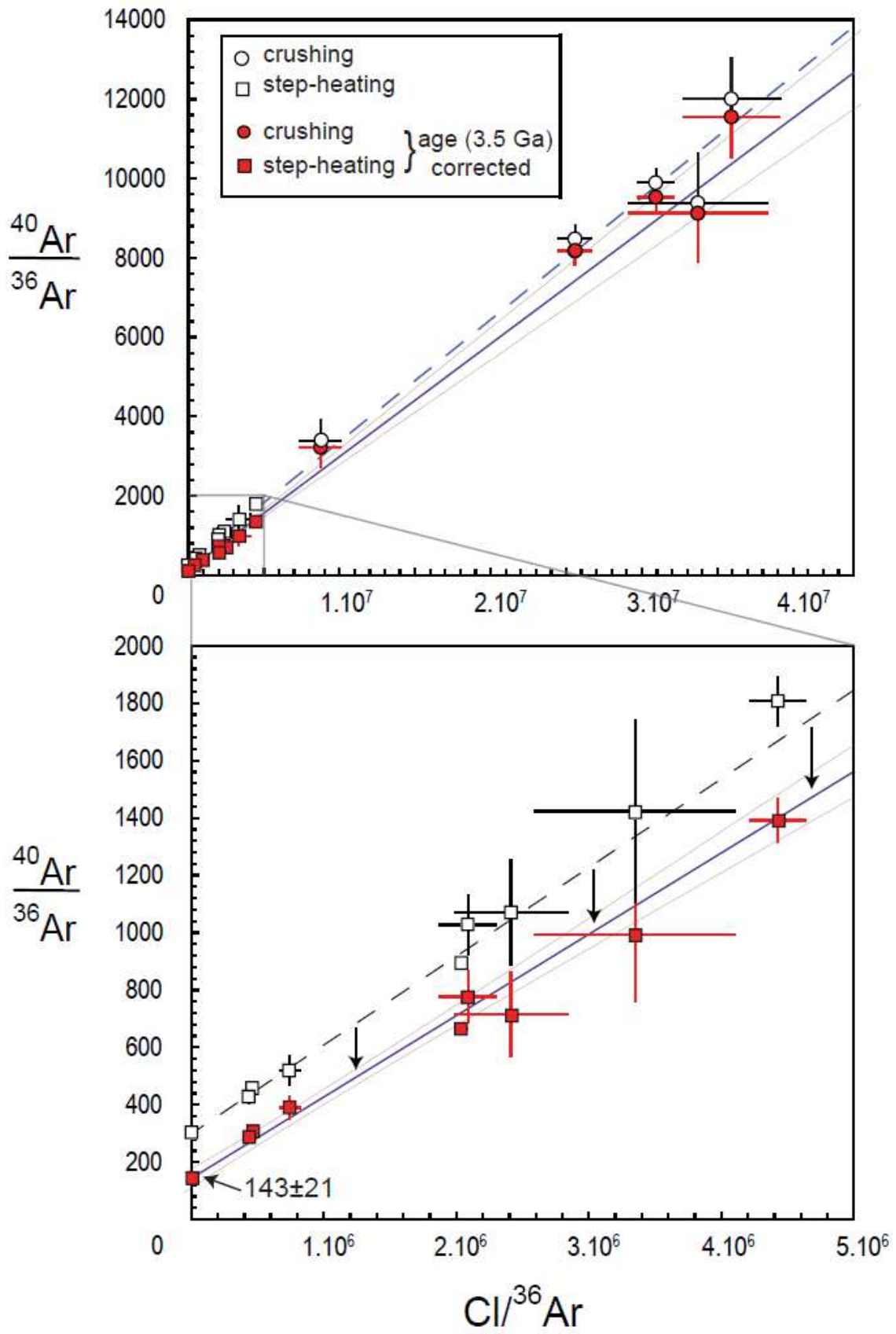
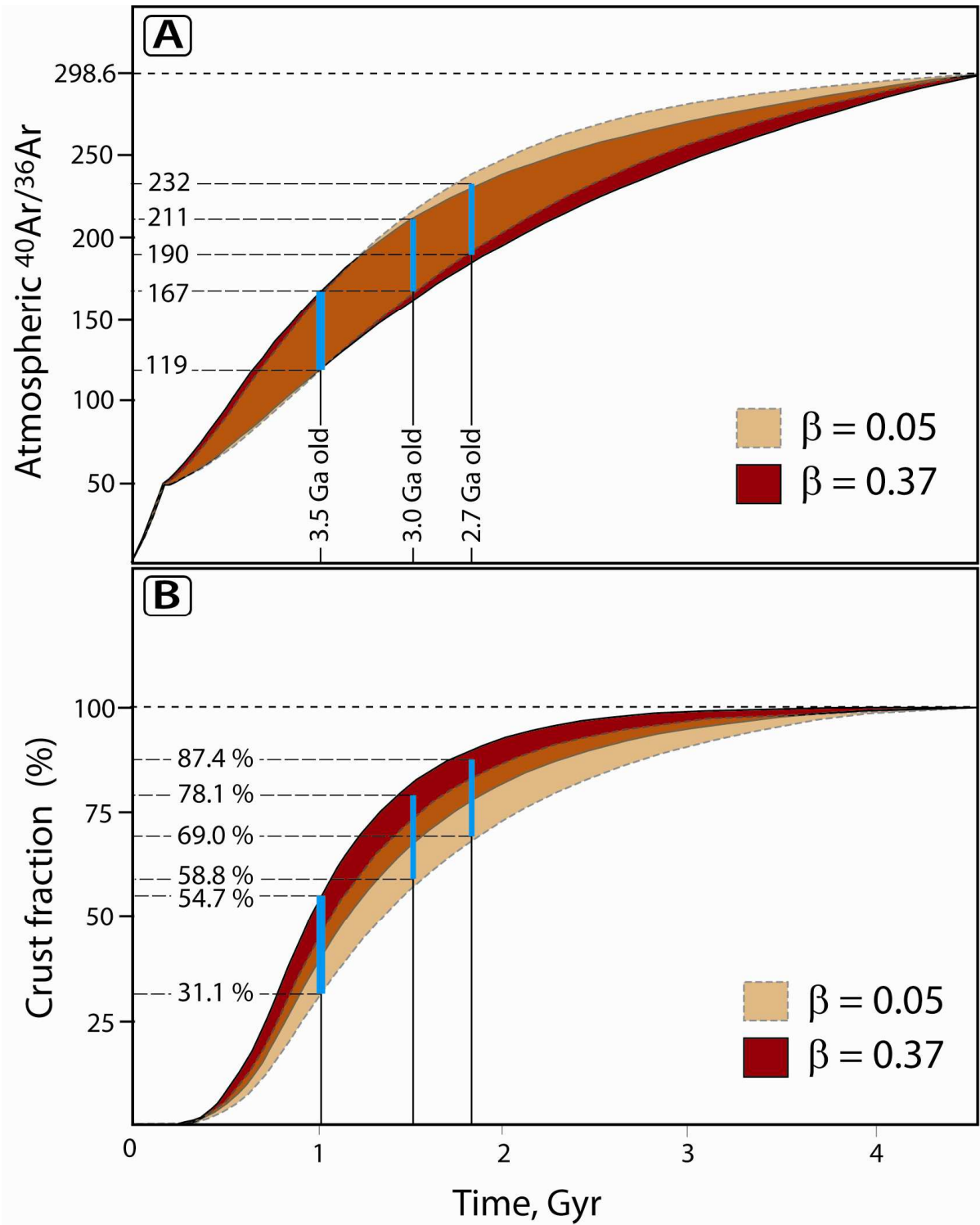


Figure 1



315

316

317

318

Figure 2

319

320 **Methods**

321 **Neutron irradiation and Ar isotope analysis**

322 The argon isotopic analysis of neutron-irradiated quartz (0.09 g), performed at
323 Manchester University, United Kingdom, was used to determine Ar, K (via $^{39}\text{Ar}_\text{K}$), Cl
324 ($^{38}\text{Ar}_\text{Cl}$), Ca ($^{37}\text{Ar}_\text{Ca}$) concentrations. Neutron irradiation of samples was carried-out in position
325 B2W of the SAFARI-1 reactor, NESCA, Pelindaba (South Africa) with a fast neutron flux of
326 $1 \times 10^{18} \text{ n/cm}^2$ as determined from Hb3gr flux monitors included in the irradiation.
327 Experimental procedures were similar to those described previously³¹. Samples were
328 progressively crushed in vacuo using modified Nupro[®] valves. Liberated gases were purified
329 using hot (400°C) Al-Zr getters before being analyzed in the mass spectrometer. Samples of
330 crushed residue were stepped heated in a Ta-resistance furnace using several temperature
331 steps, each of 30 min duration. One low temperature step at 200 °C was used to remove
332 adsorbed atmospheric noble gases from the samples. Sequential temperature steps at 200°C
333 intervals between 400-1600°C were used to extract argon from the quartz. The argon is most
334 likely to be contained in microscopic fluid inclusions, because the siliceous matrix does not
335 contain appreciable amount of noble gases²³. For both crushing and stepped heating isotopic
336 measurements were made using the MS1 mass spectrometer using a Faraday detector for Ar
337 isotope measurements. Average furnace hot blanks (1800°C) were $4 \times 10^{-13} \text{ mol}$ of ^{40}Ar . Data
338 were corrected for mass discrimination, radioactive decay since irradiation and minor neutron
339 interference corrections obtained from irradiated salts. Concentrations of K, Ca and Cl were
340 determined from samples using Hb3gr monitor data²³.

341

342 **Fluid composition**

343 Gases released by step crushing reveal the composition of a hydrothermal component
344 having a Cl/K molar ratio between 3.7 and 9.4, with elevated $^{40}\text{Ar}/^{36}\text{Ar}$ ratio. The range of
345 Cl/K is within hydrothermal end-member values found for large fluid inclusions analyzed by
346 Foriel et al. (ref. 22) (Figure A1). Gases released by crushing have lower argon isotope and
347 Cl/K (<2) ratios. $^{40}\text{Ar}/^{36}\text{Ar}$ and Cl/K correlate, indicating that the low $^{40}\text{Ar}/^{36}\text{Ar}$ component (i)
348 cannot result from dilution of an hydrothermal component by air because of the correlated
349 variation of the Cl/K ratio; and (ii) cannot be mixing with seawater (Cl/K = 57 for modern

seawater) because the latter would result in an inverse correlation between $^{40}\text{Ar}/^{36}\text{Ar}$ and Cl/K.

Statistical constraints on the age of trapped fluids

The correlations shown in Fig. 1 use the data given in Table A1 (Supplementary Information). In order to derive the initial $^{40}\text{Ar}/^{36}\text{Ar}$ ratio which we propose to be that of the atmosphere at the time of fluid trapping, data need to be corrected for in situ production, and the age of trapped fluids is critical. In the main text we have given several geological and geochemical arguments that these fluids are Archaean in age, here we further analyze the present data.

Argon-40 ($^{40}\text{Ar}_{\text{TOT}}$) trapped in fluid inclusions and in the matrix is a mixture of three components : in-situ produced ^{40}Ar ($^{40}\text{Ar}_{\text{IS}}$) since closure of the sample, atmospheric ^{40}Ar ($^{40}\text{Ar}_{\text{ATM}}$) trapped at the time of closure, and inherited argon from the hydrothermal fluid ($^{40}\text{Ar}_{\text{HY}}$).

$$^{40}\text{Ar}_{\text{TOT}} = ^{40}\text{Ar}_{\text{HY}} + ^{40}\text{Ar}_{\text{IS}} + ^{40}\text{Ar}_{\text{ATM}}$$

In gases extracted by crushing, $^{40}\text{Ar}_{\text{TOT}}$ is dominated by hydrothermal $^{40}\text{Ar}_{\text{HY}}$ and $^{40}\text{Ar}_{\text{ATM}}$ represent only a few percent of total ^{40}Ar . This can be verified for the most extreme conditions, by computing the maximum $^{40}\text{Ar}_{\text{IS}}$ contribution assuming a maximum age of 3.5 Ga and a $^{40}\text{Ar}_{\text{ATM}}$ content obtained by multiplying the observed ^{36}Ar by the modern value of $(^{40}\text{Ar}/^{36}\text{Ar})_{\text{ATM}}$ (298.6). This is a non-realistic case because it is not possible for both conditions to apply, however it demonstrates that even in the most extreme case $^{40}\text{Ar}_{\text{HY}}$ is ≥ 95 % of total ^{40}Ar .

The $\text{Cl}/^{40}\text{Ar}_{\text{TOT}}$ value of the crushing steps represents the ratio in the hydrothermal fluid end-member at better than 95%. We assume that the $\text{Cl}/^{40}\text{Ar}$ ratio of the hydrothermal end-member is the same for the crushing runs as for the step-heating runs. The assumption is justified by the fact that the data identify a single hydrothermal end-member having a constant $\text{Cl}/^{40}\text{Ar}$ ratio, e.g., in a $^{40}\text{Ar}/^{36}\text{Ar}$ vs. $\text{Cl}/^{36}\text{Ar}$ diagram. Thus we correct $^{40}\text{Ar}_{\text{TOT}}$ extracted by step-heating for the $^{40}\text{Ar}_{\text{HY}}$ contribution, using the mean $(\text{Cl}/^{40}\text{Ar}_{\text{TOT}})$ value of the crushing runs. In practice, we subtract from stepheating $^{40}\text{Ar}_{\text{TOT}}$ the measured stepheating Cl ($\text{Cl}_{\text{stepheating}}$) multiplied by the mean $(\text{Cl}/^{40}\text{Ar})_{\text{crushing}}$ ratio:

$$(^{40}\text{Ar}_{\text{TOT}})_{\text{stepheating}} = (^{40}\text{Ar}_{\text{HY}})_{\text{stepheating}} + (^{40}\text{Ar}_{\text{IS}})_{\text{stepheating}} + (^{40}\text{Ar}_{\text{ATM}})_{\text{stepheating}}$$

$$\Leftrightarrow [(^{40}\text{Ar}_{\text{IS}})_{\text{stepheating}} + (^{40}\text{Ar}_{\text{ATM}})_{\text{stepheating}}] = (^{40}\text{Ar}_{\text{TOT}})_{\text{stepheating}} - \text{Cl}_{\text{stepheating}} / (\text{Cl}/^{40}\text{Ar}_{\text{TOT}})_{\text{crushing}}$$

In order to be independent from the age and from the initial $(^{40}\text{Ar}/^{36}\text{Ar})_{\text{ATM}}$ value, we calculated the $(\text{Cl}/^{40}\text{Ar}_{\text{HY}})$ ratios of the crushing steps by correcting $^{40}\text{Ar}_{\text{TOT}}$ from the (small) contributions of $^{40}\text{Ar}_{\text{ATM}}$ and $^{40}\text{Ar}_{\text{IS}}$ for ages varying between 0 and 3.5 Ga and $(^{40}\text{Ar}/^{36}\text{Ar})_{\text{ATM}}$ ratios varying between 100 and 298.6. For all these conditions, the $(\text{Cl}/^{40}\text{Ar}_{\text{HY}})$ ratio varies between 3100 and 3300, which is well within the standard deviation of 330 among the 4 crushing data (computed with data from Table A1). We obtain $(\text{Cl}/^{40}\text{Ar})_{\text{HY}} = 3245$ (mean of all these conditions) ± 330 (standard deviation for the four crushing steps). ^{40}Ar from stepheating runs consists now of a mixture of in-situ produced $^{40}\text{Ar}_{\text{IS}}$ and atmospheric $^{40}\text{Ar}_{\text{ATM}}$. For each step, we computed the amount of $^{40}\text{Ar}_{\text{IS}}$ as :

$$(^{40}\text{Ar}_{\text{IS}})_{\text{stepheating}} = [(^{40}\text{Ar}_{\text{IS}})_{\text{step heating}} + (^{40}\text{Ar}_{\text{ATM}})_{\text{stepheating}}] - (^{36}\text{Ar}_{\text{ATM}})_{\text{stepheating}} \times (^{40}\text{Ar}/^{36}\text{Ar})_{\text{ATM}}$$

(where $[(^{40}\text{Ar}_{\text{IS}})_{\text{step heating}} + (^{40}\text{Ar}_{\text{ATM}})_{\text{stepheating}}]$ has been computed as above). Since we do not know a priori $(^{40}\text{Ar}/^{36}\text{Ar})_{\text{ATM}}$, we consider this ratio as an input parameter for which we assume different values, in practice varying it between 100 and 298.6. With the obtained $(^{40}\text{Ar}_{\text{IS}})_{\text{stepheating}}$, we compute the corresponding ages as we also have K concentration for each step.

Thus for each $(^{40}\text{Ar}/^{36}\text{Ar})_{\text{ATM}}$ input value, we obtain a set of stepheating data and we test statistically the homogeneity of ages between the different steps. For that, we computed the Ar-Ar plateau (using the Isoplot software developed by K. Ludwig, http://bgc.org/isoplot_etc/isoplot.html) corresponding to each $(^{40}\text{Ar}/^{36}\text{Ar})_{\text{ATM}}$ value (Table A3). The best solutions are those for which ages have the lowest standard deviation and the mean square weighted deviation (MSWD) value closest to 1 (meaning that the errors can account for the spread of data), as given in Table A3 and illustrated in Fig. A2, and correspond to ages close to the formation age of 3.5 Ga. For ages lower than 3 Ga, the MSWD value becomes rapidly close to 0 and the standard deviations increase dramatically. This, together with an age of 3.0 Ga obtained for a previously analysed quartz sample (for which the in-situ produced ^{40}Ar was dominant and the hydrothermal contribution was constant for all steps, so that direct Ar-Ar plateau ages could be obtained²⁷) as well as with the geological and morphological evidence discussed earlier, points to a paleo-Archaeon age for fluids trapped in quartz, probably the formation age, and excludes a young age for trapped fluids.

Xenon isotopic signature

Xenon isotope analysis was done at CRPG Nancy, France. Pure quartz grains (1-2 mm in size) were selected and ultrasonically cleaned with acetone. After cleaning, 0.2-0.8 g of the quartz sample was loaded into a stainless steel tube for crushing. The tube was then baked overnight at 150°C under high vacuum to desorb atmospheric noble gases from the sample surface before extraction. The sample was crushed at room temperature by activating a piston 1000 times. During crushing, condensable gases including xenon were trapped in a glass cold-finger immersed in liquid nitrogen to separate them from lighter noble gases (He, Ne, Ar). After cryogenic separation, the non-trapped fraction was rapidly pumped, condensable gases were desorbed, and Xe was purified using five successive getters cycled between 700°C and room temperature. Xe isotopes were then analyzed by static mass spectrometry.

The Xe isotope abundances (Figure A3, Table A2), normalized to ^{132}Xe and to the isotopic composition of xenon in modern air, display excesses at masses 126 and 131 (Figure A3-a), comparable to excesses reported by Srinivasan³³ for an Archaean barite sample, and attributed by this author to cosmic ray spallation reactions forming ^{126}Xe , and production of ^{130}Ba (n,γ) ^{131}Xe by epithermal neutrons^{27,33,34}. Interaction with cosmic rays is consistent with the location of the present sample at the surface. Not only ^{126}Xe and ^{131}Xe isotopes are in excess relative to ^{132}Xe , but also are other lighter Xe isotopes including ^{130}Xe and ^{129}Xe . ^{130}Xe is itself in excess of ^{129}Xe , indicating the contribution of the natural radioactivity of ^{130}Ba ($^{130}\text{Ba}(2\text{EC})^{130}\text{Xe}$, with a half life of $6.0 \pm 1.1 \times 10^{20} \text{ a}$ ²⁷) and therefore the presence of an old xenon component. Thus the heavy isotopes of xenon ($^{132,134,136}\text{Xe}$) must also be contributed by products of the natural fission of ^{238}U and the original Xe isotope composition has to be corrected. The U content was measured in these samples (Service d'Analyse des Roches et des Minéraux, CRPG Nancy, France) by two different methods (light leaching of powders to obtain an average U content of fluid inclusions, and U measurement of quartz before any crushing) which both gave a similar U concentration of 0.15 ppm. In Figure A3-b, the heavy isotope abundances of Xe are corrected for contribution of fissiogenic Xe during 3.5 Ga (using the younger fluid ages of 3.0 or 2.7 Ga results in a smaller but essentially comparable corrections, Fig. A3-b). The corrected Xe abundance is clearly deficient in heavy Xe isotopes ($\sim 1\%/amu$) compared to modern air. Such depletion, found previously in well dated samples like 3.5 Ga barite and 3.0 Ga quartz^{33, 27, 28} is proposed to represent the Xe isotope composition of Archaean air.

Building of the model

We used a 3 reservoir (mantle crust and atmosphere), first order rate, box model similar to the one developed by Hamano & Ozima⁹ (Figure A4). In such a model, the mantle contained initially primordial noble gases (here, ^{36}Ar) that were subsequently degassed into the atmosphere. However, atmospheric noble gases might have been contributed by sources other than mantle degassing, e.g., late accretion of volatile-rich bodies. In this case, the model, although conceptually different, yields essentially the same results. Indeed it does not make a mathematical difference between an early catastrophic event that injects mantle-derived ^{36}Ar into the atmosphere before production of significant ^{40}Ar , and the occurrence of a ^{36}Ar -bearing atmosphere, with later contribution of ^{40}Ar from the mantle. Note that the early degassing event is required by all models based on Ar isotopes, to account for the large $^{40}\text{Ar}/^{36}\text{Ar}$ contrast between the mantle and the atmosphere⁹. ^{40}Ar is only produced from the radioactive decay of ^{40}K , with a half life of 1.25 Ga. Potassium, initially in the mantle, has been extracted together with Ar, during mantle melting (we assume that both Ar and K are highly incompatible during mantle melting, which is well established in the case of K, and well supported by experimental data for Ar³¹). Ar degasses into the atmosphere and a fraction of K is transferred in the crust (resulting in 20-50 % bulk silicate Earth potassium being stored in the crust nowadays). ^{40}Ar produced in the crust partly degasses (see next paragraph). Thus, ^{40}Ar originates from both the mantle and the crust, and its flux into the atmosphere will depend on mantle convection/degassing and also on the volume of crust that stores K. The computations were carried out with the Stella[®] code. Data used to build this model and constrain its solutions are presented in Table A4.

The mantle convection rate impacts directly on the degassing of Ar and on the storage of K in the crust through felsic crust production. In order to mimic the decrease of heat in Earth, especially that due to radioactivity, an exponential decrease of mantle convection is classically assumed⁹. However, such an exponential decrease is not sufficient to explain the modern high $^{40}\text{Ar}/^{36}\text{Ar}$ difference between the present-day mantle and atmosphere, so that an early catastrophic degassing event is required that occurred in the first ~100-200 Ma. Such an early high convection rate is independently supported by extinct radionuclides⁴⁰⁻⁴². Different durations of catastrophic degassing have been tested and a time interval of 170 Ma gives the largest numbers of solutions. Thus degassing rates can be separated in two parts: before 170 Ma during the intense degassing with a constant rate, and after 170 Ma with the exponential decrease of degassing. A fraction of radiogenic argon generated in the crust degasses into the

atmosphere, with a degassing coefficient taken as variable between 5% and 50 %, the last number corresponding to a comparison between Rb-Sr and K-Ar ages for crustal rocks⁹. The model is run with variable atmospheric $^{40}\text{Ar}/^{36}\text{Ar}$ ratios constrained by the present quartz data at the different periods of time defined above: $t = 3.5$ Ga, $^{40}\text{Ar}/^{36}\text{Ar} = 119\text{-}167$; $t = 3.0$ Ga, $^{40}\text{Ar}/^{36}\text{Ar} = 167\text{-}211$; and $t = 2.7$ Ga, $^{40}\text{Ar}/^{36}\text{Ar} = 190\text{-}232$. The crustal growth curves obtained with these different closure ages are indistinguishable (Figure 2), which means that these results are not model-dependent within the 2.7-3.5 Ga range.

The solutions of our Ar-based model evolution of the continental crust indicate that about half of the present-day continental crust was already present 3.5 Ga ago (range : 31-55 %) and that at our lower age limit of 2.7 Ga, the crustal volume was 69-88 % of the present-day felsic crust. Our continental crust growth curves (Fig. A5) are intermediate between those representing early and intense growth in the Hadean^{1,3,43} and those representing late^{4,44} or sigmoidal growths^{5,45}. They predict a larger crustal volume in the Hadean than the model based on U-Pb or Hf isotope compositions of zircons. However, these geochemical proxies integrate crustal reworking, which can be corrected for by combining these data with oxygen isotopes¹. In such a case our model runs are consistent with those derived from U-Pb, Hf and O isotopes of continental zircons, that is, high crustal production in the Archaean, followed by a factor of ~2-4 reduction of the net growth rate beginning at ~ 3.0 Ga ago (same position of the inflection, Fig. A5).

- 496 31. Kendrick, M.A., Burgess, R., Pattick, R.A.D. & Turner, G. Halogen and Ar-Ar age
497 determinations of inclusions within quartz veins from porphyry copper deposits using
498 complementary noble gas extractions. *Chem. Geol.* **177**, 351-370 (2001).
- 499 32. Basford, J. R., Dragon, J.C., Pepin, R.O., Coscio, M.R. & Murthy, V.R. Krypton and
500 Xenon in Lunar fines. *Proc. Lunar Sci. Conf. 4th*, 1915-1955 (1973).
- 501 33. Srinivasan, B. Barites: anomalous xenon from spallation and neutron-induced reactions.
502 *Earth Planet. Sci. Lett.* **31**, 129-141 (1976).
- 503 34. Meshik, A.P., Hohenberg, C.M., Pravdivtseva, O.V. & Kapusta, Ya.S. Weak decay of
504 ^{130}Ba and ^{132}Ba : Geochemical measurements. *Phys. Rev. C - Nucl. Phys.* **64**, 352051-352056
505 (2001).
- 506 35. Ballentine, C.J., van Keken, P.E., Porcelli, D. & Hauri, E.H. Numerical models,
507 geochemistry and the zero paradox noble-gas mantle. *Phil. Trans. R. Soc. A.* **360**, 2611–2631
508 (2002).
- 509 36. Burnard, P., Graham, D. & Turner, G. Vesicle-specific noble gas analyses of "popping
510 rock": Implications for primordial noble gases in earth. *Science* **276**, 568-571 (1997).
- 511 37. Moreira, M., Kunz, J. & Allègre, C. J. Rare gas systematics in popping rock: isotopic and
512 elemental compositions in the upper mantle. *Science* **279**, 1178-1181 (1998).
- 513 38. Trieloff, M. The Nature of Pristine Noble Gases in Mantle Plumes. *Science* **288**, 1036-
514 1038 (2000).
- 515 39. Mukhopadhyay, S. Early differentiation and volatile accretion recorded in deep-mantle
516 neon and xenon. *Nature* **486**, 101-104 (2012).

40. Heber, V.S., Brooker, R.A., Kelley, S.P., & Wood, B.J. Crystal-melt partitioning of noble gases (helium, neon, argon, krypton, and xenon) for olivine and clinopyroxene. *Geochim. Cosmochim. Acta* **71**, 1041-1061 (2007).
41. Boyet, M. & Carlson, R. W. ^{142}Nd evidence for early (>4.53 Ga) global differentiation of the silicate Earth. *Science* **309**, 576-581 (2005).
42. Caro, G., Bourdon, B., Birk, J. L. & Moorbath, S. ^{146}Sm - ^{142}Nd evidence from Isua metamorphosed sediments for early differentiation of Earth's mantle. *Nature* **423**, 428-432 (2003).
43. Fyfe, W. S. Evolution of the Earth's crust: modern plate tectonics to ancient hot spot tectonics? *Chem. Geol.* **23**, 89 (1978).
44. Hurley, P. M. Absolute abundance and distribution of Rb K and Sr in the Earth. *Geochim. Cosmochim. Acta* **32**, 273 (1968).
45. Veizer, J. & Jansen, S.L. Basement and sedimentary recycling and continental evolution. *J. Geol.* **87**, 341-370 (1979).